Sizing and Control of a Hybrid Ship Propulsion System Using Multi-Objective Double-Layer Optimization

XUEZHOU WANG [ID] [1], **(Member, IEEE), UDAI SHIPURKAR** [2], **ALI HASELTALAB** [1],
HENK POLINDER [ID] [1], **(Senior Member, IEEE), FRANS CLAEYS** [3], **AND RUDY R. NEGENBORN** [ID] [1]

[1]Department of Maritime and Transportation Technology, Delft University of Technology, 2628 CD Delft, The Netherlands
[2]Maritime Research Institute Netherlands (MARIN), 6708 PM Wageningen, The Netherlands
[3]GEOxyz, 8550 Zwevegem, Belgium

Corresponding author: Xuezhou Wang (x.wang-3@tudelft.nl)

ABSTRACT Ship hybridization has received some interests recently in order to achieve the emission target by 2050. However, designing and optimizing a hybrid propulsion system is a complicated problem. Sizing components and optimizing energy management control are coupled with each other. This paper applies a nested double-layer optimization architecture to optimize the sizing and energy management of a hybrid offshore support vessel. Three different power sources, namely diesel engines, batteries and fuel cells, are considered which increases the complexity of the optimization problem. The optimal sizing of the components and their corresponding energy management strategies are illustrated. The effects of the operational profiles and the emission reduction targets on the hybridization design are studied for this particular type of vessel. The results prove that a small emission reduction target of about 10% can be achieved by improving the diesel engine efficiency using the batteries only while the achievement of a larger emission reduction target mainly depends on the amount of the hydrogen and/or on-shore charging electricity consumed. Some design guidelines for hybridization are derived for this particular ship which could be also valid for other vessels with similar operational profiles.

INDEX TERMS Hybrid, offshore support vessel, sizing, control, energy management.

I. INTRODUCTION

Climate change policies are creating significant restrictions on greenhouse gas emissions in the transportation industry [1]. The shipping emissions occupies from 2.76% in 2012 to 2.89% in 2018 in the global anthropogenic greenhouse gas emissions [2]. This industry section is under great pressure to meet the emission target of at least 50% reduction by 2050 [2]. Electrification is one of the promising ways to reduce CO_2 emissions. Therefore, hybrid and electric vessels have received a lot of interest recently.

Fig. 1 shows some common propulsion systems of hybrid and electric ships in practice. The well-known mechanical propulsion systems are widely adopted for ship applications. Based on the original mechanical propulsion systems,

The associate editor coordinating the review of this manuscript and approving it for publication was Shuaihu Li [ID].

the diesel-electric propulsion systems are then applied to decouple the power generation and power consumption [3]. The operating point of the diesel generator can even be decoupled from the rotational speed of the main shaft by using a DC bus [4], [5] which finally increases the efficiencies of the diesel engines. The electric propulsion systems have been developed quickly after the batteries, especially lithium-ion (Li-ion) batteries, are integrated into the propulsion systems [6], [7]. Recently, hydrogen fuel cells have attracted interest because of their relatively high energy density [8] and completely emission-free [9], [10]. They have been widely investigated for automotive applications [11], [12]. However, they are barely studied for marine applications [10], [13]. Several different types of hydrogen fuel cells for maritime applications are reviewed in [14]. Low temperature polymer electrolyte membrane fuel cell (PEMFC) is most promising for ships with mission requirements up to a dozen hours [14].
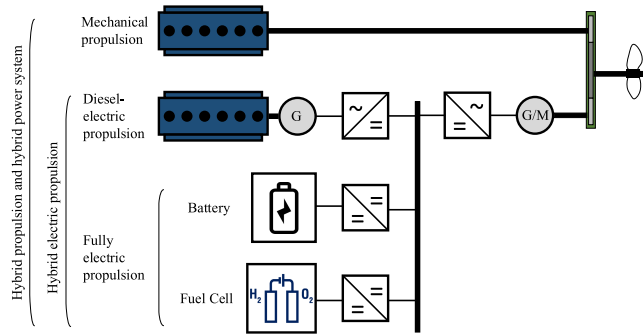
FIGURE 1. Overview of propulsion systems.

FIGURE 2. System level optimization architectures [20].

High temperature fuel cells like solid oxide fuel cell (SOFC) can achieve higher overall system efficiencies. However, SOFC has not yet been fully ready for maritime applications due to its poor dynamic performance [15]. Fig. 1 also shows the hybrid propulsion system in which the propeller is driven by different types of movers and/or the electrical system is supplied by different power sources [16]. The hybrid propulsion system provides more flexible operation modes, such as power take off, power take in, and power take home [17]. The detailed benefits of hybridization have been investigated for eight types of vessels with various operational profiles [18].

However, on the other hand, the hybridization results in a more complicated design and optimization for the propulsion system. The design process is a multi-objective optimization problem that spreads over topology [19], sizing, and control (energy management). Fortunately, for automotive industry, the system level optimization strategies have been well studied and applied to electric vehicle applications [20]. Fig. 2 shows the optimization architectures which are widely used in automotive industry. The most popular optimization architecture is the control design (the inner layer) nested within the plant design (the outer layer). The most differences between different double-layer optimizations are the algorithms applied to those two layers. An exhaustive search method is adopted for the plant design problem at the early stage [21] while multi-objective genetic algorithm (GA) or particle swarm optimization (PSO) is more suitable to handle a very large design space [22], [23]. For the control design problem in the inner layer, the dynamic programming (e.g. mixed-integer linear programming (MILP)) is more promising to find the optimal control policy [24] than the traditional rule-based (RB) algorithm [22].

Back to the marine applications, Table 1 lists several references working on sizing and energy management of power sources. For instance, several objectives like fuel consumption, gensets start/stop numbers, and running hours were formulated into one single objective [25]. This might miss the trade-off among different objectives. A complicated three-stage optimization with a single objective for each stage is applied to optimize all-electric ship power systems in [27]. However, only the control problem is addressed for a given ship power plant design in which the power rating and the
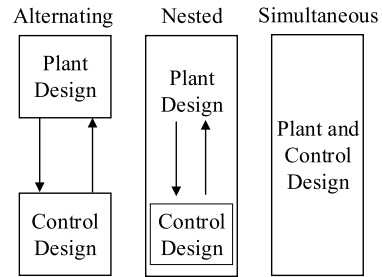
energy storage capacity have been known from the beginning. The optimal generator sizing and its management are studied by using a GA in [28]. This sizing problem is not that complicated since only one power source is considered. Two-stage optimization with single objective is adopted to optimize the battery size of an electric ferry ship [29]. But all the constraints are just formulated linearly and the problem is then solved by the *fmincon* function in MATLAB rather than other more advanced algorithms. One thing needs to be mentioned is that not all of the available algorithms are listed in Table 1. A more complete overview, but for automotive applications, can be found in [20]. Some recent literature [32] presents the optimization of the energy conversion scheme for off-grid applications which might be also interesting to ship applications.

Reviewing all the above mentioned studies highlights two facts. The first one is that more power sources like diesel engines, diesel gensets, batteries and fuel cells complicate the powertrain design for hybrid ships. The second one is that the system level optimization architectures developed for automotive applications could be tried to solve the design problem for marine applications [32].

This project aims to look into the feasibility of the hydrogen based ship hybridization for several different types of ships, as well as the effect of hybridization on the reduction of CO_2 emissions. This paper presents a part of our current work on applying a multi-objective double-layer optimization methodology to sizing and control of a hybrid ship propulsion system. The contribution of this paper is firstly to formulate the developed methodology and show its effectiveness to find out the optimal solutions based on some certain objectives. This case study is carried out on an offshore support vessel with specific operational profiles. Therefore, the second contribution is to derive some design guidelines of hydrogen based hybridization for ships with similar operational profiles.

This paper starts with a brief introduction of the studied offshore support vessel. The ship parameters, the operational profiles, and the proposed hybrid propulsion system are explained. Next, the procedure of the double-layer optimization is illustrated followed by formulating the optimization objectives and constraints. Subsequently, the hybrid propulsion systems are optimized using the proposed methodology for four different operational profiles. The influences of the

TABLE 1. Summary from the review of hybrid/electric ships.

| | Objective | Algorithms | | Power sources | | |
		Component sizing	Energy management	Engine/Genset	Battery	Fuel cells
Skjong *et al.* [25]	Single	-	MILP	✓	✓ / -	-
Shang *et al.* [26]	Multi	-	NSGA-II	✓	✓	-
Kanellos *et al.* [27]	Single	-	DP+PSO	✓	✓	-
Boveri *et al.* [28]	Single	GA	-	✓	-	-
Mashayekh *et al.* [29]	Single	MATLAB *fmincon*		✓	✓	-
Skinner *et al.* [30], [31]	Multi	GA	RB/SQP	✓	-	-
Banaei *et al.* [10]	Single	-	MILP	-	✓	✓
This paper	Multi	NSGA-II	MILP	✓	✓	✓

GA: genetic algorithm; NSGA-II: non-dominated sorting genetic algorithm II; PSO: particle swarm optimization; DP: dynamic programming; MILP: mixed-integer linear programming; RB: rule-based; SQP: sequential quadratic programming.

operational profiles and the emission reduction targets on the hybridization design are discussed. Finally, conclusions are drawn.

II. VESSEL DESCRIPTIONS AND ASSUMPTIONS
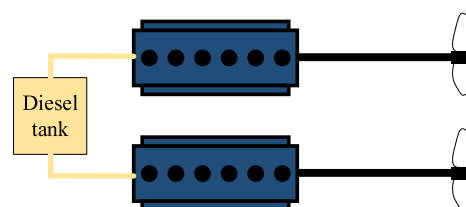
A. SHIP PARAMETERS

The studied vessel is an offshore support vessel as shown in Fig. 3. Table 2 gives the basic parameters of the vessel. Fig. 4(a) shows the original mechanical propulsion system. All the needed energy is provided by the diesel fuel which is stored in tanks. Two fixed pitch propellers are driven by two diesel engines. They have the same power rating of 720 kW for each. Fig. 5 shows the propeller curve of the original mechanical propulsion system with high-speed diesel engines. There should be a reduction gearbox locating
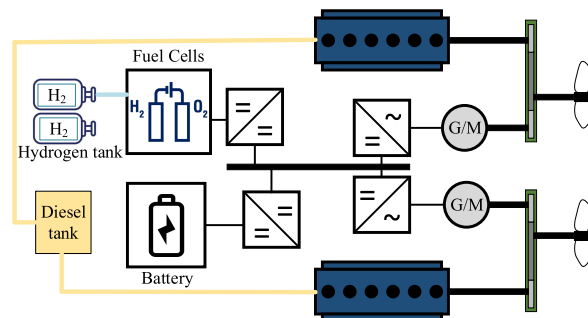

(a) Original mechanical propulsion powertrain

(b) Initial proposed hybrid propulsion powertrain

FIGURE 4. Propulsion powertrain studied.

between the engine and the propeller. It is just omitted in Fig. 4(a) for simplicity. The auxiliary loads are supplied by a separate diesel generator which will not be considered in this study.

B. HYBRID PROPULSION AND OPERATIONAL MODES

The existing propulsion system is considered to be hybridized to achieve the emission target. On-shore electricity could be charged in batteries and used for propulsion. Li-ion batteries are adopted due to their high power/energy density compared to other types of batteries [33]. Hydrogen could be another energy source for zero CO_2 emission. The hydrogen storage could be in the form of liquid hydrogen, compressed hydrogen or metal hydrides [15]. The first two options are more common in practice. The liquid hydrogen is adopted in this case study considering its relatively higher energy density.

FIGURE 3. The studied offshore support vessel (photo by GEOxyz).

TABLE 2. Parameters of the studied vessel.

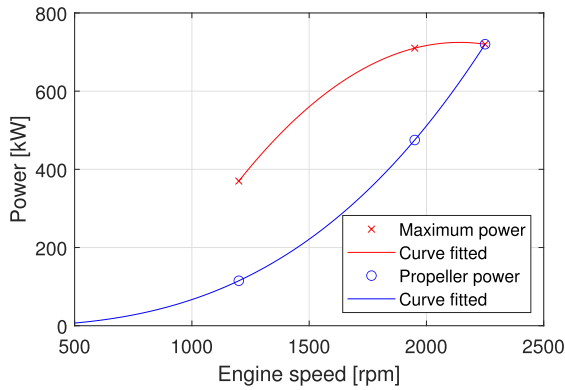| Description	Unit	Value
Type		Offshore support
Overall length	[m]	19.5
Width	[m]	7.5
Main engines power	[kW]	720
Specific fuel consumption	[g/kWh]	214
Maximum speed	[knots]	24
Cruising speed	[knots]	22

FIGURE 5. Propeller curve of the original mechanical propulsion.

As mentioned above, PEMFC is adopted because it operates at relatively low temperatures and widely available in current commercial markets. Fig. 4(b) gives the proposed hybrid propulsion system according to the ship builder's experience. The system contains the energy storage systems including diesel and hydrogen tanks and one set of batteries. It also contains two diesel engines, two electric motors/generators and fuel cells for energy conversion.

The diesel engines and the electric motors can drive the propellers independently or in a combined way according to the power demand. The motors can be supplied by the batteries or the fuel cells separately or simultaneously based on the energy management strategy. The motors can also operate as electric generators to take the excess power delivered from the engines to the propellers. The batteries can charge or discharge through a bi-directional DC/DC converter.

C. OPERATIONAL PROFILES

Originally, this offshore support vessel is used for crew transfer mission. The corresponding operational profiles of the power demand are measured from the main diesel engines on two different days and given in Fig. 6. The total traveling period is about 12 hours. The vessel takes around 1.5 hours to arrive at the working area and then stays there for about 7 hours. Finally, it takes 1.5 hours to return. As we could see from Fig. 6, the maximal power happens when the ship goes to and returns from the working area. There is a small amount of power required in the working area. One thing might be good to mention here is the power peaks in Fig. 6(a). They are probably random operations because of the different captains
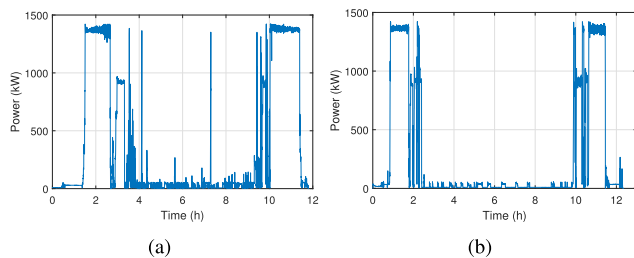

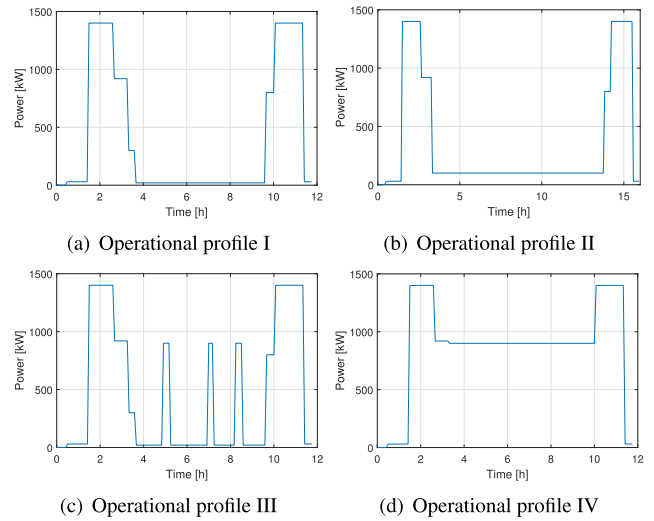**FIGURE 6. Operational profile measured on-site.**

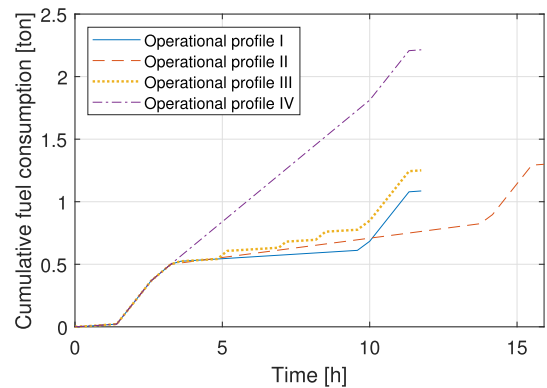**FIGURE 7. Operational profiles studied.**

FIGURE 8. Diesel fuel consumption with mechanical propulsion.

since there are no peaks in Fig. 6(b). In order to be consistent with other operational profiles studied in this paper, Fig. 6 is simplified to operational profile I as shown in Fig. 7(a). The dynamic characteristics in the time scale of a couple of seconds are not considered in the following optimization.

This offshore support vessel may have different operational missions which correspond to different operational profiles. One objective of this paper is to investigate the effects of operational profiles on the hybrid powertrain design. Fig. 7 gives the studied operational profiles. The vessel is assumed to have the same going and returning voyages, but different missions in the middle. As mentioned above, operational profile I represents the original measured one. This indicates the operational mission with low power and energy demand in the working area. Operational profile II has slightly higher power demand and longer traveling time. It represents the mission with relatively low power demand, but high energy demand. Fig. 7(c) shows operational profile III which is exactly the same as the profile I, but with three power peaks in the middle. This indicates some fast, but short, moving in the working area. This profile represents the mission with short-time high power demand, but relatively low energy demand. The survey

vessel has a similar operational profile shown in Fig. 7(d). It travels at a medium speed in the working area for a survey task. This operational profile IV represents the mission with high power and energy demand.

By using the method developed in Section III-B, the diesel fuel consumption with the original mechanical propulsion system is predicted for these four operational profiles and given in Fig. 8. They are the reference points for the following optimization.

III. OPTIMIZATION DEFINITION

This section will firstly introduce the proposed optimization procedure. The objectives, the variables, and the constraints of the optimization will then be formulated. Subsequently, the estimation of the diesel fuel and the liquid hydrogen consumption will be explained.

A. OPTIMIZATION PROCEDURE

Fig. 9 gives the optimization procedure applied in this paper. The whole process is a nested architecture in which every evaluation of a plant needs a full optimization of the control design. The input parameters include the operational profiles and the parameters of components, such as the quantity, the power/energy rating and the C-rates of battery charging and discharging. Some other operating limitations can also be as inputs, for example, the initial state-of-charge (SOC) of battery and the operating range of fuel cells.
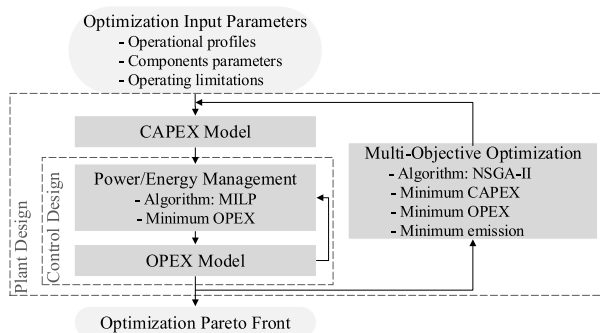

FIGURE 9. Optimization procedure.

With the quantities and power/energy rating of the components, the outer layer could roughly estimate the CAPEX of the proposed propulsion powertrain. In the inner layer, the energy management strategy is optimized to minimize the OPEX. The start/stop number, the running time and the corresponding power of the components are scheduled using the MILP algorithm. It is a linear programming algorithm with an objective function and inequality and/or equality constraints in which the variables are integers [34], [35]. The consumption of the diesel fuel and the liquid hydrogen is predicted in the OPEX model. The non-dominated sorting genetic algorithm II (NSGA-II) is applied to determine Pareto optimal solutions for this multi-objective problem [26], [36].

It is a well-known evolutionary based algorithm [37]. The first population of N propulsion designs is generated and evaluated by the CAPEX and OPEX models taking the energy management strategy into account. Each design varies based on a set of input variables provided. All N propulsion designs are evaluated according to the optimization objectives, and a new generation of N propulsion designs is generated from the best (fittest) individuals of the previous generation. In this study, the population size N and the generations are both selected as 100.

B. OPTIMIZATION VARIABLES AND OBJECTIVES

The variables and the objectives of the double-layer optimization will be introduced separately as follows:

TABLE 3. Fixed parameters of the studied vessel.

Description	Machine parameter	Value
Number of diesel engines	N_{DE}	2
Number of battery set	N_{Bat}	1
Number of fuel cell set	N_{FC}	1
Diesel fuel price [$/kg]	C_{DF}	1.45
On-shore electricity price [$/kWh]	C_e	0.16
H_2 purchasing price [$/Liter]	C_{H_2}	0.2
kWh to kg conversion coefficient for H_2	K_{E-m}	0.03
kg to liter conversion coefficient for H_2	K_{m-V}	24.8
Cost per kW of diesel engines [$/kW]	C_{DE}	300
Cost per kW of batteries [$/kW]	C_{Bat}	475
Cost per kW of fuel cells system [$/kW]	C_{FC}	2000

TABLE 4. Variables of NSGA-II.

Description	Variables	Value min	max
Power rating of diesel engines [kW]	P_{DE}^r	0	2000
Energy rating of batteries [kWh]	E_{Bat}^r	0	5000
Power rating of fuel cells [kW]	P_{FC}^r	0	2000

1) OUTER LAYER OPTIMIZATION

Table 3 gives the fixed parameters of the optimization. In this paper, the numbers of diesel engines, batteries, and fuel cells are determined based on the powertrain selected in Fig. 4(b). Table 4 gives the variables of the studied propulsion system. There are three objectives to be minimized simultaneously in the outer layer optimization. They are the CAPEX, the OPEX and the weight of the diesel fuel consumed M_{DF} which are formulated by (1), (2) and (3), respectively.

$$OF_1^{GA} = CAPEX(P_{DE}^r, E_{Bat}^r, P_{FC}^r, N_{DE}, N_{Bat}, N_{FC}), \quad (1)$$

where OF_1^{GA} is the objective function of the CAPEX in the outer layer, P_{DE}^r, E_{Bat}^r, P_{FC}^r are power/energy rating given in Table 4, N_{DE}, N_{Bat}, N_{FC} are the number of power sources given in Table 3.

$$OF_2^{GA} = OPEX(M_{DF}, V_{H_2}) + OPEX_{Bat}, \quad (2)$$

where OF_2^{GA} is the objective function of the OPEX, the first item is the cost of the diesel and hydrogen fuel and the second

item is the cost of the on-shore charging electricity.

$$OF_3^{GA} = M_{DF}(P_{DE}, N_{DE}, X_{DE}). \qquad (3)$$

where OF_3^{GA} is the objective function of the weight of the consumed diesel fuel calculated by (6). The diesel fuel consumption actually indicates the emission reduction by comparing it to the reference point shown in Fig. 8.

TABLE 5. Variables of MILP.

Description	Variables	Piecewise approx.
Diesel engines power	P_{DE}^i	$P_{DE_1}^i, P_{DE_2}^i, P_{DE_3}^i$
Batteries power	P_{Bat}^j	-
Fuel cells power	P_{FC}^k	$P_{FC_1}^k, P_{FC_2}^k, P_{FC_3}^k$
Diesel engines binary variable	X_{DE}	$X_{DE_1}^i, X_{DE_2}^i, X_{DE_3}^i$
Batteries binary variable	X_{Bat}	-
Fuel cells binary variable	X_{FC}	$X_{FC_1}^i, X_{FC_2}^i, X_{FC_3}^i$

2) INNER LAYER OPTIMIZATION

Table 5 gives the variables of the inner layer optimization. They are the power of each component and binary variable related at each time interval. For the binary variable, 1 indicates the component switches on and 0 means off. The objective of the inner layer is to minimize the OPEX given by (4) in which the cost of the on-shore charging electricity in the batteries is not considered. This is because the batteries always discharge till the minimal SOC at the end to minimize the diesel and hydrogen fuel consumption for a given powertrain.

$$OF^{LP} = OPEX(M_{DF}, V_{H_2}), \qquad (4)$$

$$OPEX = \sum_{t=0}^{H} \left(C_{DF} \sum_{i=1}^{N_{DE}} M_{DF}^i(t) + C_{H_2} \sum_{k=1}^{N_{FC}} V_{H_2}^k(t) \right), \qquad (5)$$

where

$$M_{DF}^i(t) = f_{DF}(P_{DE}^i(t)) \Delta t \cdot X_{DE}(t), \qquad (6)$$

$$V_{H_2}^k(t) = f_{FC}(P_{FC}^k(t)) \Delta t \cdot K_{E-m} K_{m-V} \cdot X_{FC}(t), \qquad (7)$$

in which $f_{DF}(P_{DE}^i(t))$ is a function of the fuel consumption rate with respect to the instantaneous power, $f_{FC}(P_{FC}^k(t))$ is a function relating the output power to the total power generated by fuel cells, K_{E-m} and K_{m-V} are conversion coefficients relating the power generated to the consumed hydrogen.

The diesel fuel consumption $M_{DF}^i(t)$ can be then predicted by $P_{DE}^i(t)$. It is assumed that only the steady-state diesel fuel consumption is considered while the transient influence is not taken into account. The fuel consumption is calculated using the simple analytical engine torque model given in [38]. The engine torque is modeled as a function of the fuel consumption m_f^* and engine speed n_{DE}^* in the form of a second-order Taylor expansion of two variables given in (8). It is in a normalized expression in which the superscript '*'

represents the ratio between the actual value and the nominal value.

$$T_{DE}^* = 1 - c_1(1 - n_{DE}^*) + c_2(1 - n_{DE}^*)^2 - c_3(1 - m_f^*) + c_4(1 - m_f^*)^2 + 2c_5(1 - n_{DE}^*)(1 - m_f^*), \qquad (8)$$

where c_1-c_5 are parameters which determine the trend of the engine output torque. These five parameters can be calculated with five measurements on the real diesel engine. If there is no actual information, these parameters could be roughly estimated by implementing five typical operation points given in Table 6. Fig. 10 then shows the normalized specific fuel consumption. This empirical model can then be applied to estimate the fuel consumption rate by multiplying the specific fuel consumption by power. The typical fuel consumption rate curve of diesel engines is given in Fig. 11. It indicates this curve can be approximated by a quadratic function given

TABLE 6. Parameters for torque estimation.

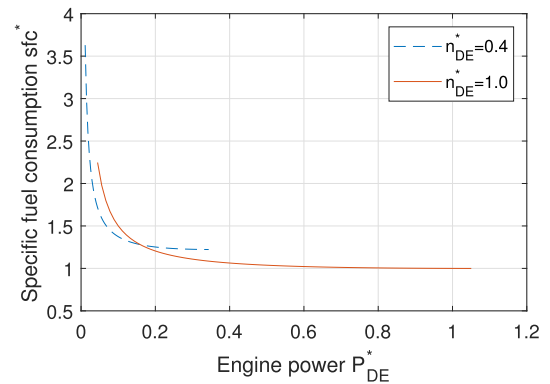| Operational points	n_{DE}^*	m_f^*	T_{DE}^*
1	1	0.5	0.48
2	1	0.06	0
3	0.75	0.5	0.49
4	0.5	0.25	0.2
5	0.5	0.04	0

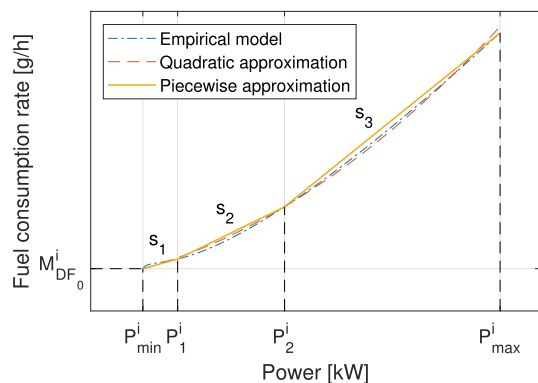**FIGURE 10. Normalized specific fuel consumption.**

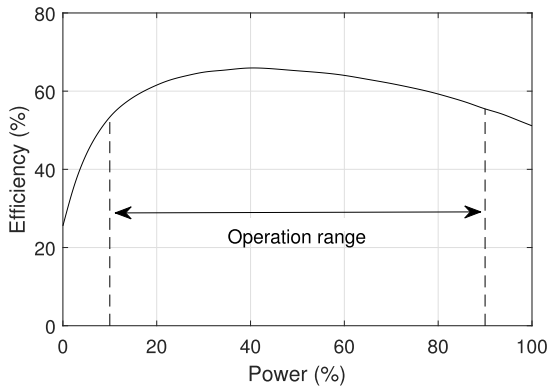**FIGURE 11. Typical curve of fuel consumption rate of DEs.**
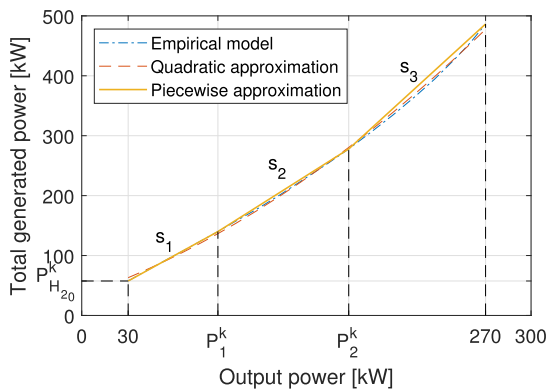
FIGURE 12. Typical efficiency of fuel cell systems.

FIGURE 13. Total generated power with respect to output power of a FC.

by:

$$f^i_{DF}(P^i_{DE}(t)) = \alpha_i \left(P^i_{DE}(t) \right)^2 + \beta_i P^i_{DE}(t) + \gamma_i, \qquad (9)$$

where α_i, β_i and γ_i are coefficients of the fitted quadratic function.

It is not straightforward to calculate the hydrogen volume required for generating each kWh electric energy since the fuel cell system is complicated. The temperature, the pressure, and even the aging all affect the performance of the fuel cell system. Therefore, the equation (7) applies the conversion coefficients to related the power generated and the hydrogen consumed [10]. However, not all of the power generated by the fuel cells delivers to the loads, but disappears in the form of losses. Fig. 12 gives a typical efficiency of a fuel cells system which describes the function of $f_{FC}(P^k_{FC}(t))$ [10]. Fig. 13 gives an example of the total power generated with respect to the output power of a fuel cells system whose rated power is 300 kW. Similar to Fig. 11, the original curve can be approximated by a quadratic function given by (10) [27].

$$f^k_{FC}(P^k_{FC}(t)) = \alpha_k \left(P^k_{FC}(t) \right)^2 + \beta_k P^k_{FC}(t) + \gamma_k, \qquad (10)$$

where α_k, β_k and γ_k are coefficients of the fitted quadratic function.

However, MILP can only deal with linear problems rather than quadratic functions like (9) and (10). The easiest way is to apply piecewise linear functions to get over this quadratic function [39]. Three segments are adopted in this paper as shown in Fig. 11 and 13. s_1, s_2 and s_3 are the slopes for three segments, respectively. The analytical representations of f^i_{DF} and f^k_{FC} will be re-formulated by using the piecewise linear approximation. For brevity, the detailed formulations can be found in the appendix.

C. OPTIMIZATION CONSTRAINTS

Each diesel engine should not provide a higher power than its rating. This constraint can be formulated as:

$$0 \leq P^i_{DE}(t) \leq P^r_{DE}. \qquad (11)$$

Similarly, the batteries have a power constraint as:

$$P^{r,c}_{Bat} \leq P^j_{Bat}(t) \leq P^{r,dc}_{Bat}, \qquad (12)$$

where $P^j_{Bat}(t)$ is either a positive value (discharging mode) or a negative value (charging mode). By doing this, there is no need to apply additional binary variables to prevent simultaneous charging and discharging for an individual set of batteries [10]. Moreover, it is critical to increase the lifetime of the batteries by keeping the SOC within an acceptable range (0.25 - 0.85 in this paper) as:

$$SOC_{min} \leq SOC^j(t) \leq SOC_{max}, \qquad (13)$$

where

$$SOC^j(t) = SOC^j(t-1) - \frac{P^j_{Bat}(t) \cdot X^j_{Bat}(t)\Delta t}{E^r_{Bat}}. \qquad (14)$$

Fig. 12 gives a typical efficiency of a fuel cells system. In practical, the system is expected to operate between the range of 10% and 90% of its rated output power due to the high efficiency. This leads to the following constraint for the fuel cells.

$$0.1 \cdot P^r_{FC} \leq P^k_{FC}(t) \leq 0.9 \cdot P^r_{FC}. \qquad (15)$$

Finally, the total power generation and consumption should be balanced during the operation period. This can be formulated as:

$$P_L(t) = \sum_{i=1}^{N_{DE}} P^i_{DE}(t) \cdot X^i_{DE}(t) + \sum_{j=1}^{N_{Bat}} P^j_{Bat}(t) \cdot X^j_{Bat}(t)$$
$$+ \sum_{k=1}^{N_{FC}} P^k_{FC}(t) \cdot X^k_{FC}(t). \qquad (16)$$

The left side of (16) represents the total power demand based on the operational profile given in Fig. 6. The right side represents the power generated by the diesel engines, the discharging or charging power by batteries and the power supplied by the fuel cells, respectively. For brevity, the detailed formulations of these constraints using the piecewise linear approximation are updated in the appendix.

The weights and volumes of the propulsion system are also critical to be constrained in practice. However, they are assumed not to be constrained in this case study since this paper aims to look into the ideal design of the hybrid propulsion system with a large emission reduction range.

IV. RESULTS AND DISCUSSIONS

A. OPTIMIZED PARETO FRONTS

The proposed propulsion systems are optimized according to the above four operational profiles. Fig. 14 gives the Pareto fronts of the diesel fuel consumption with respect to the CAPEX. In general, the diesel fuel consumption goes down when the CAPEX increases. This can be easily explained by the involvements of the batteries and fuel cells which are more expensive than the diesel engines. Another thing we could observe from Fig. 14 is that the case with operational profile II reduces the diesel consumption more effectively than the other three scenarios at the beginning. This will be explained in the following section.
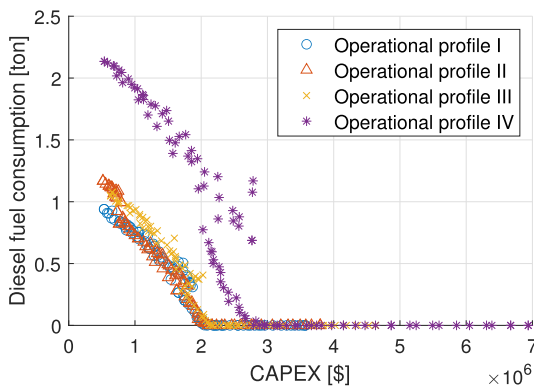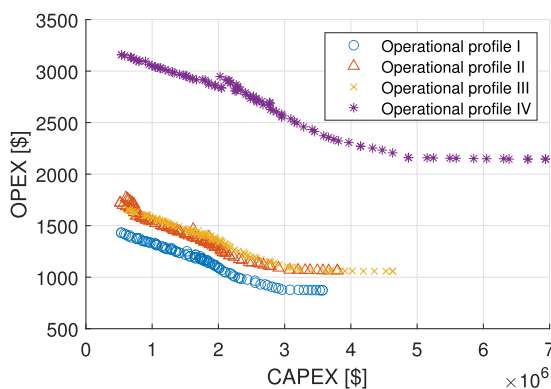

FIGURE 14. Diesel fuel consumption vs. CAPEX.

FIGURE 15. OPEX vs. CAPEX.

Fig. 15 shows the OPEX with respect to the CAPEX for all scenarios. The OPEX presented here only includes the cost of the diesel fuel, the hydrogen, and the on-shore charging electricity for a one-way route. No maintenance and depreciation costs are considered. The OPEX may vary with different unit prices in different markets. This paper will not discuss the OPEX further, but shows the trade-off between the OPEX

and the CAPEX. Electrical power sources have less operation and maintenance costs than traditional diesel engines which might lead to an interesting investigation from the economic perspective.

Instead of giving the total CAPEX, Fig. 16 shows the power rating of the diesel engines and fuel cells and the energy rating of the batteries for different operational profiles. At first glance, the trends are similar for all four situations. The diesel engines become smaller while the fuel cells and the batteries become bigger when the diesel fuel consumption decreases. However, the detailed sizing and design guidelines are different depending on the operational profiles and the emission reduction targets.

B. SMALL EMISSION REDUCTION

The small emission reduction discussed here is about 10% compared to the original mechanical propulsion systems. Fig. 16 indicates that the power ratings of the fuel cells are very small below 10% emission reduction. It actually means that the fuel cells may not be necessary for the emission reduction by 10%, at least for this case study. This could simplify the practical hybrid propulsion systems if only diesel engines and batteries are considered.

In order to prove the above statement, the propulsion systems with diesel engines and batteries are optimized using the same methodology developed in the previous section. Fig. 17 shows the comparison results of the optimized fronts with and without the fuel cells. In each case, two fronts coincide on the left which means it is more practical to only involve the batteries for a small emission reduction target. However, this is not valid for a higher reduction above 10% in this case study. The hybrid propulsion systems with both batteries and fuel cells are more promising for higher emission reduction targets.

Table 7 summaries the optimal solutions from the Pareto fronts for the ~10% emission reduction target. Fig. 18 shows the power schedules of the selected design for each operational profile. For all scenarios, the batteries support a part of the power for the going and returning trips in order to lower the size of the diesel engines. For operational profiles I and III, the batteries provide the whole power between 4 h and 10 h except the diesel engines support three power peaks for operational profile III. For operational profiles II and IV, they may lead to huge batteries if only the batteries provide the power within the working area. Therefore, it can be observed from Fig. 18(b) and (d) that the diesel engines and the batteries operate alternatively. Although the frequency of the alternate operation for profile II is higher than that for profile IV, the similar idea behind is to make the diesel engines run at high power which finally results in higher efficiencies.

Fig. 19 shows the diesel engine efficiencies of the original mechanical propulsion system. Except for operational profile IV, the diesel engines operate a lot of time at low efficiencies. Fig. 20 shows the engine efficiencies of the selected
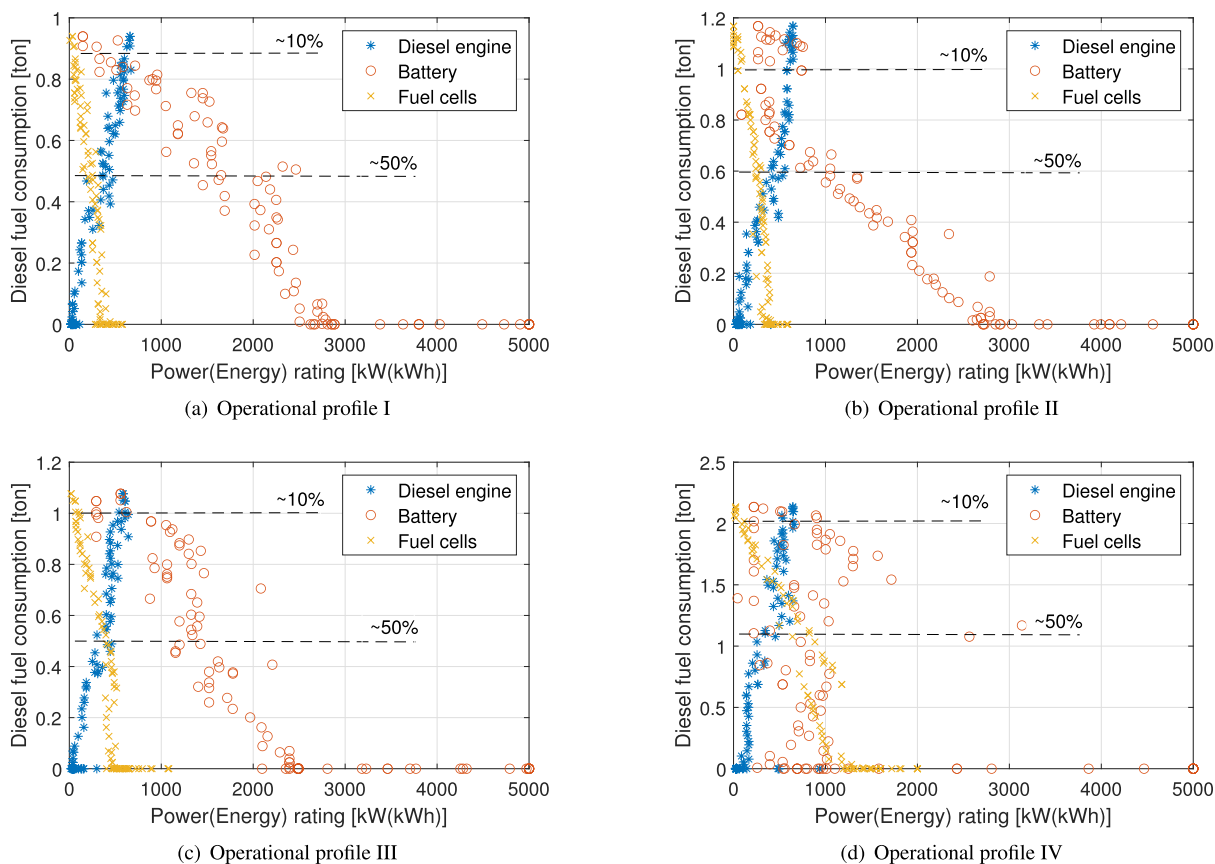
IEEE *Access*

FIGURE 16. Power rating of diesel engines, fuel cells and energy rating of batteries for different operational profiles.
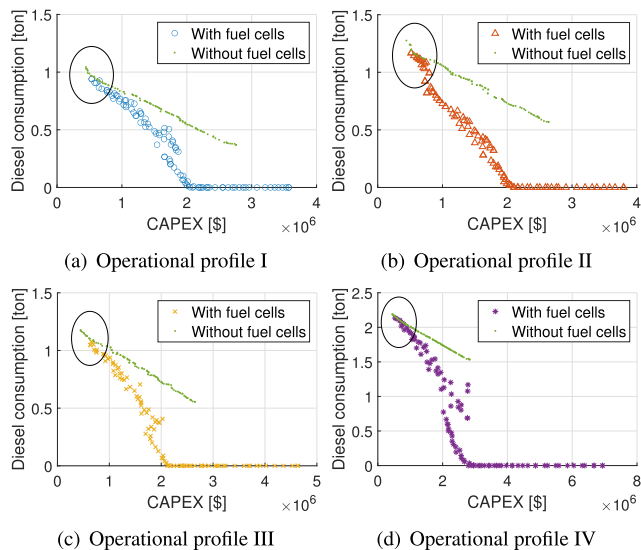

FIGURE 17. Pareto fronts without fuel cells.

TABLE 7. Solutions for small emission reduction target.

Operational Profile	P_{DE}^r [kW]	E_{Bat}^r [kWh]	CAPEX [k\$]	M_{DF} [ton]
I	628	431	582	0.95
II	638	342	545	1.15
III	585	574	624	1.10
IV	514	933	752	2.08

even though the efficiencies of the engines could be further improved. However, as mentioned in Fig. 17, adopting the fuel cells could be more cost-effective to improve the engine efficiencies further for operational profile II.

In summary, the hybrid propulsion systems including the diesel engines and the batteries are most cost-effective and practical for a small emission reduction target (e.g. ~10% in this case study). The common idea for different operational profiles is to improve the efficiencies of the diesel engines. The batteries provide all the low power for the scenarios with low energy demand and the engines only switch on to support the short-time power peaks (i.e. I and III). For the cases with high energy demand (i.e. II and IV), the diesel engines provide most of the power and energy. However, the batteries help the engines operate at higher power which leads to higher efficiencies.

hybrid propulsion systems given in Table 7. The diesel engines run at high efficiencies during most of the time when they switch on, apart from operational profile II. The selected hybrid propulsion system for profile II has already reduced the diesel fuel consumption by about 10%,

(a) Operational profile I

(b) Operational profile II

(c) Operational profile III
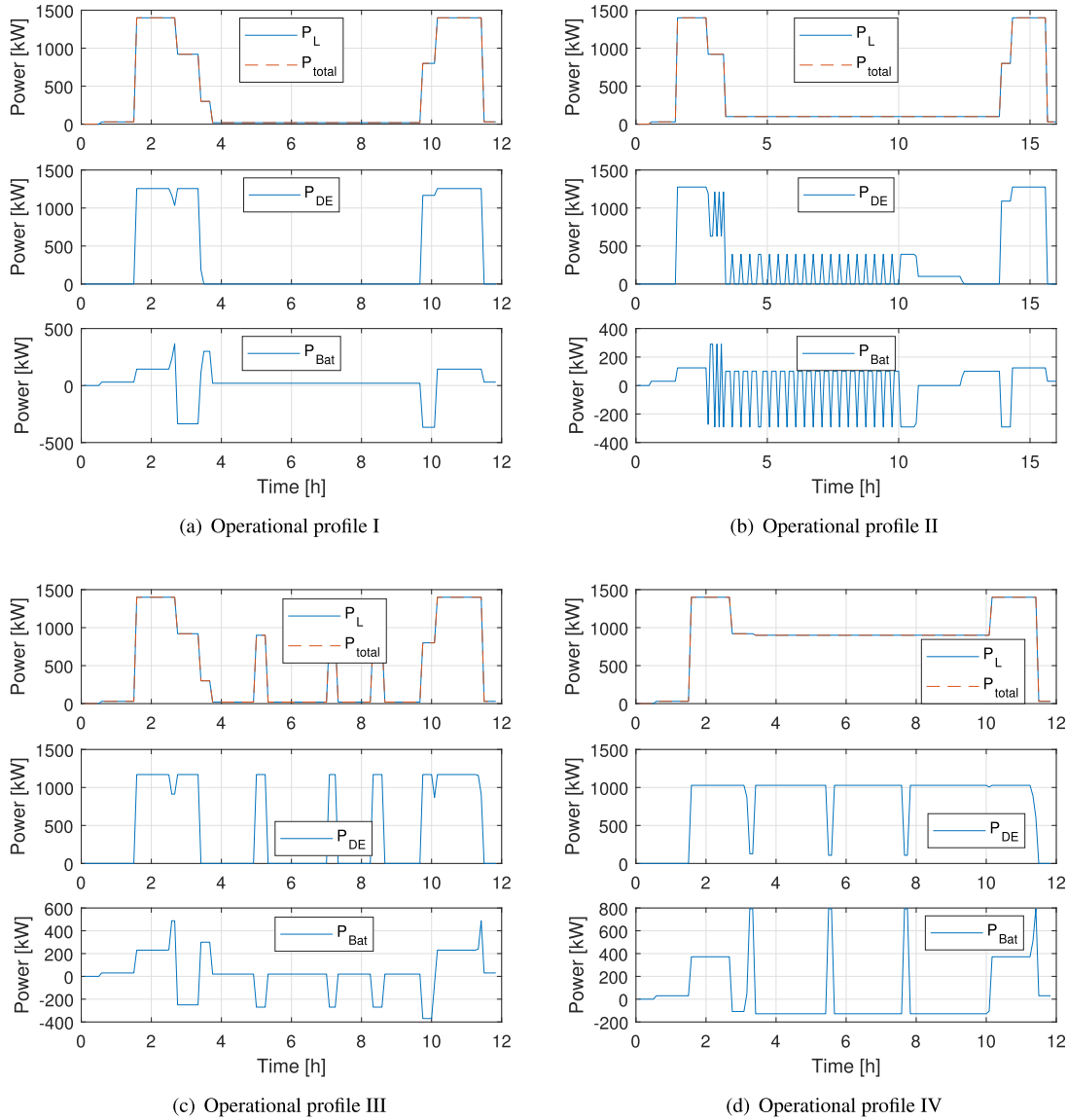
(d) Operational profile IV

FIGURE 18. Power schedule of the selected designs for small emission reduction.

C. MEDIUM EMISSION REDUCTION

The medium emission reduction discussed here is around 50% compared to the original mechanical propulsion systems. Fig. 20 has indicated that there is little space to improve the diesel engine efficiencies for operational profile I, III, and IV. Therefore, it needs a certain amount of fuel cells and large batteries to achieve this medium emission reduction target as shown in Fig. 16. One exception is the case for operational profile II. This can be explained by Fig. 20(b). The engine efficiencies could still be improved further before adopting larger fuel cells and batteries.

Table 8 summaries the optimal solutions from the Pareto fronts for the ~50% emission reduction target. The first three scenarios roughly have the similar components sizing. The fourth scenario has a larger fuel cells because its emission reduction is not mainly contributed by improving the engine efficiencies.

TABLE 8. Solutions for medium emission reduction target.

	P^r_{DE} [kW]	E^r_{Bat} [kWh]	P^r_{FC} [kW]	CAPEX [k\$]	OPEX [\$]	M_{DF} [ton]
I	363	1356	251	1364	1245	0.53
II	511	1064	210	1232	1486	0.67
III	446	1391	278	1484	1468	0.65
IV	255	731	885	2270	2810	1.03

Fig. 21 shows the power schedules of the selected design for each operational profile. For these four operational profiles, all power sources provide power together during the going and returning traveling. This helps to reduce the size of the individual components for a lower CAPEX. Moreover, the diesel engines still provide more than half of the power and energy for going and returning. Although the power ratings of the fuel cells are different for different operational
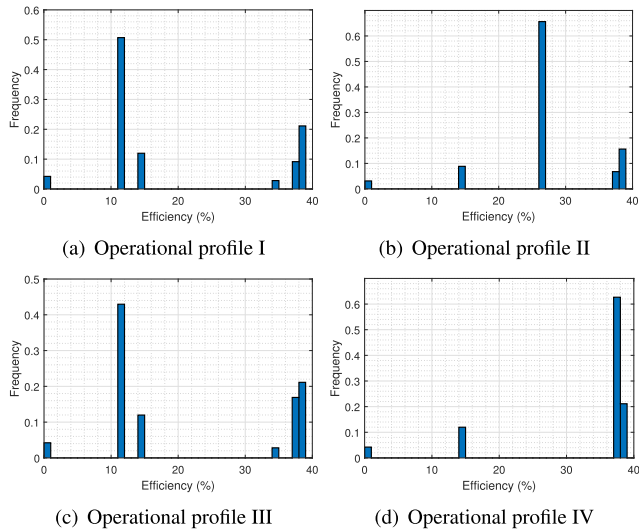
FIGURE 19. Engine efficiencies of the original mechanical propulsion systems.
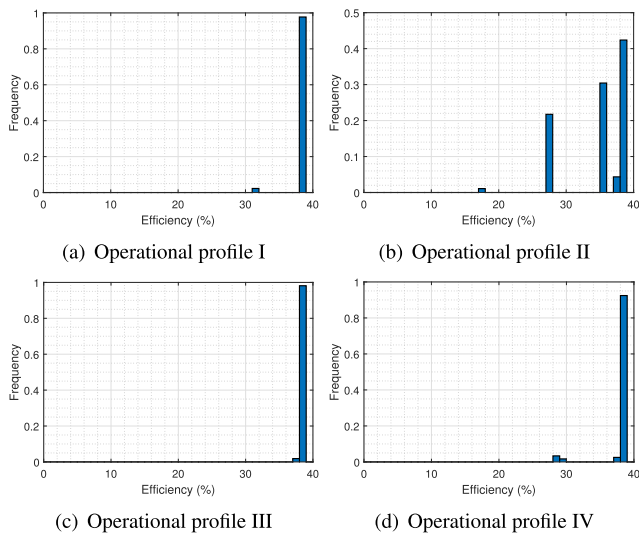

FIGURE 20. Engine efficiencies of the selected hybrid propulsion systems.

profiles, they operate roughly at a constant power level during most of the operating time in each scenario. This helps the fuel cells to operate at high efficiencies resulting in a lower OPEX. For the working area with low power demand (i.e. I and II), the diesel engines are switched off and all the power provided only by the fuel cells. The similar phenomenon happens for operational profile III. However, the short-time power peaks are supported by the batteries rather than the engines like in the previous section of small emission reduction. For the working area with high power and energy demand (i.e. IV), both the diesel engines and the fuel cells provide the power.

In summary, the hybrid propulsion systems including engines, batteries and fuel cells are more cost-effective to achieve the medium emission reduction target (e.g. ~50% in this case study). At this level, it is most likely difficult to

further improve the diesel engine efficiencies. The emission reductions mainly depend on the amount of the hydrogen and the on-shore charging electricity used for the propulsion comparing to the diesel fuel consumed. In this case study, the diesel engines and the batteries provide approximately half of the total power, respectively, for the going and returning voyages. The fuel cells provide relatively low and roughly constant power during the whole traveling. One exception is the scenario with high power and energy demand (i.e. IV). The diesel engines and the fuel cells provide roughly half of the power required in the working area for the whole voyage while the batteries support the left power for going and returning.
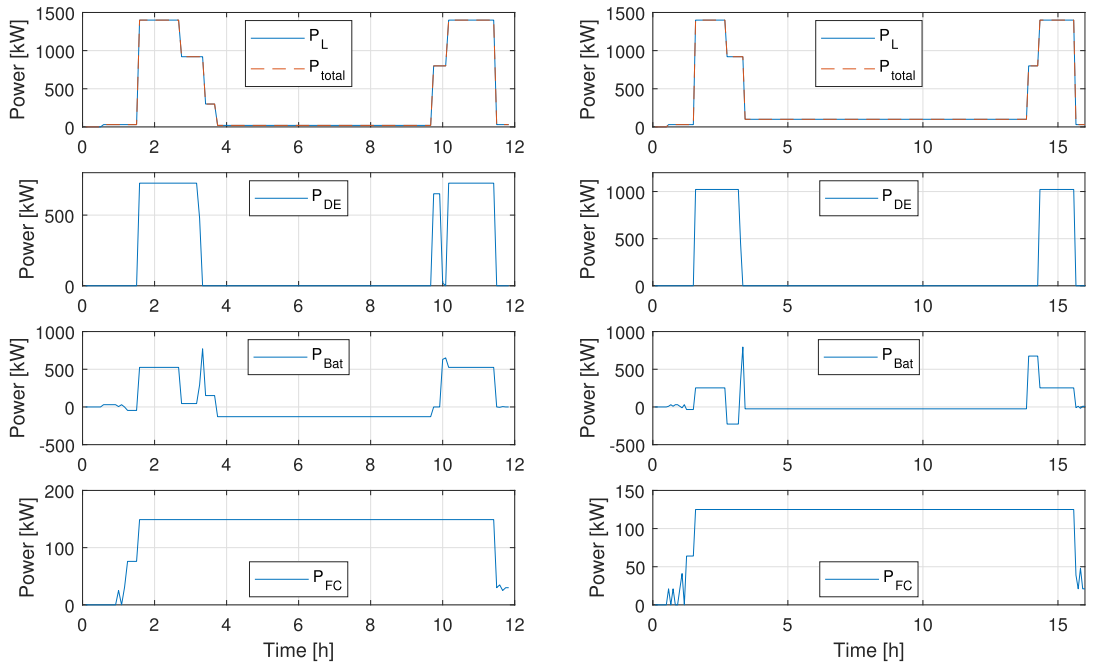
D. ULTIMATE EMISSION REDUCTION
The ultimate emission reduction discussed means the emission-free propulsion systems. Table 9 summaries the solution designs for the emission-free systems for all operational profiles. Extremely small diesel engines are still there in the results. However, they are always switched off if we check their power schedules. Therefore, it is reasonable to ignore them in the following discussion. Similar to the previous section of the medium emission reduction, the first three cases approximately have the similar sizing of the components. Compared to the fourth scenario, the first three hybrid systems have relatively smaller fuel cells, but larger batteries.

**TABLE 9.** Solutions for emission-free.

	P_{DE}^r [kW]	E_{Bat}^r [kWh]	P_{FC}^r [kW]	CAPEX [k\$]	OPEX [\$]
I	16	2654	410	2090	1052
II	24	2896	356	2102	1246
III	32	2481	484	2166	1296
IV	26	1010	1230	2955	2582

Fig. 22 gives the power schedules of the selected design for each operational profile. The first three scenarios almost follow the same pattern. The fuel cells provide a small amount (~25%) of the maximal power at the beginning and the end to lower the sizing of the batteries. The batteries provide most of the total power and follow the transient power demand for the going and returning trips. In the working area, the fuel cells provide almost the whole power apart from the batteries take over the short-time power peaks for the operational profile III. The last scenario has the opposite situation. The fuel cells provide most (~80%) of the power and energy for the going and returning trips while the batteries support some power to lower the sizing of the fuel cells. In the working area, only the fuel cells provide the whole power. Another interesting thing could be found if we compare the average power to the fuel cells power rating. The average power is 398 kW, 346 kW, 465 kW and 865 kW, respectively, for each operational profile. Apart from the last one, the first three values are close to the fuel cells power ratings given in Table 9. This fits our common feeling that the fuel cells roughly provide

(a) Operational profile I

(b) Operational profile II
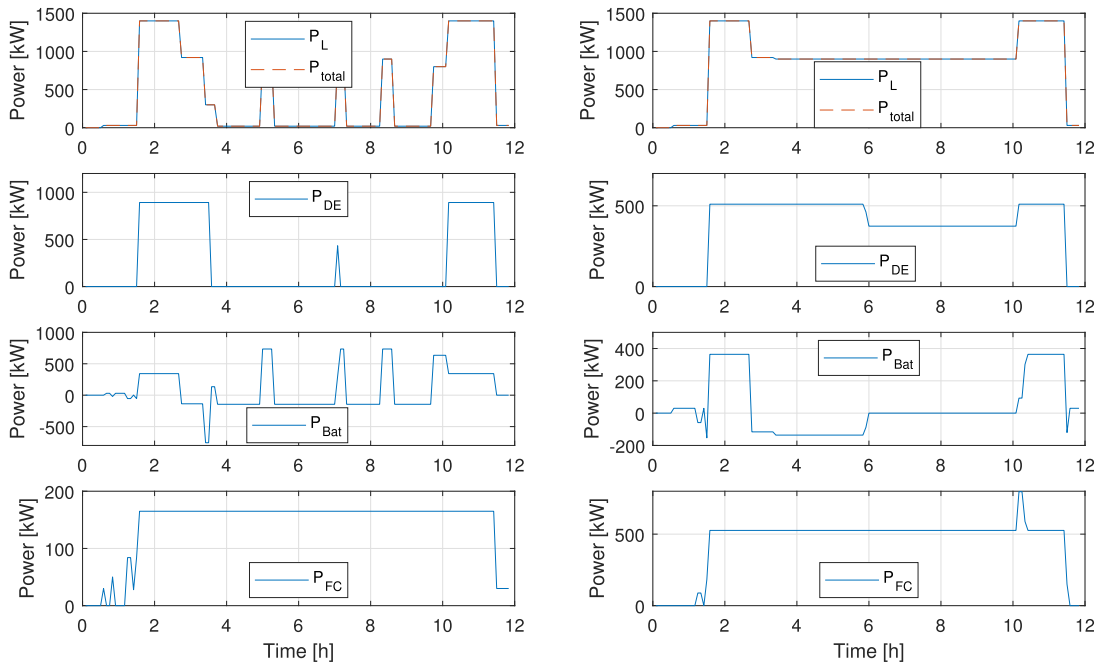
(c) Operational profile III

(d) Operational profile IV

FIGURE 21. Power schedule of the selected designs for medium emission reduction.

a long-term constant power at high efficiencies while the batteries are applied to boost the power and level the energy.

In summary, the hybrid propulsion systems including batteries and fuel cells are common for the emission-free target. In most cases, the power rating of the fuel cells could be

roughly selected based on the average power. But it could be larger for an operational profile with high power and energy demand. The battery size could then be estimated according to the maximal power and the energy demand for the whole voyage.
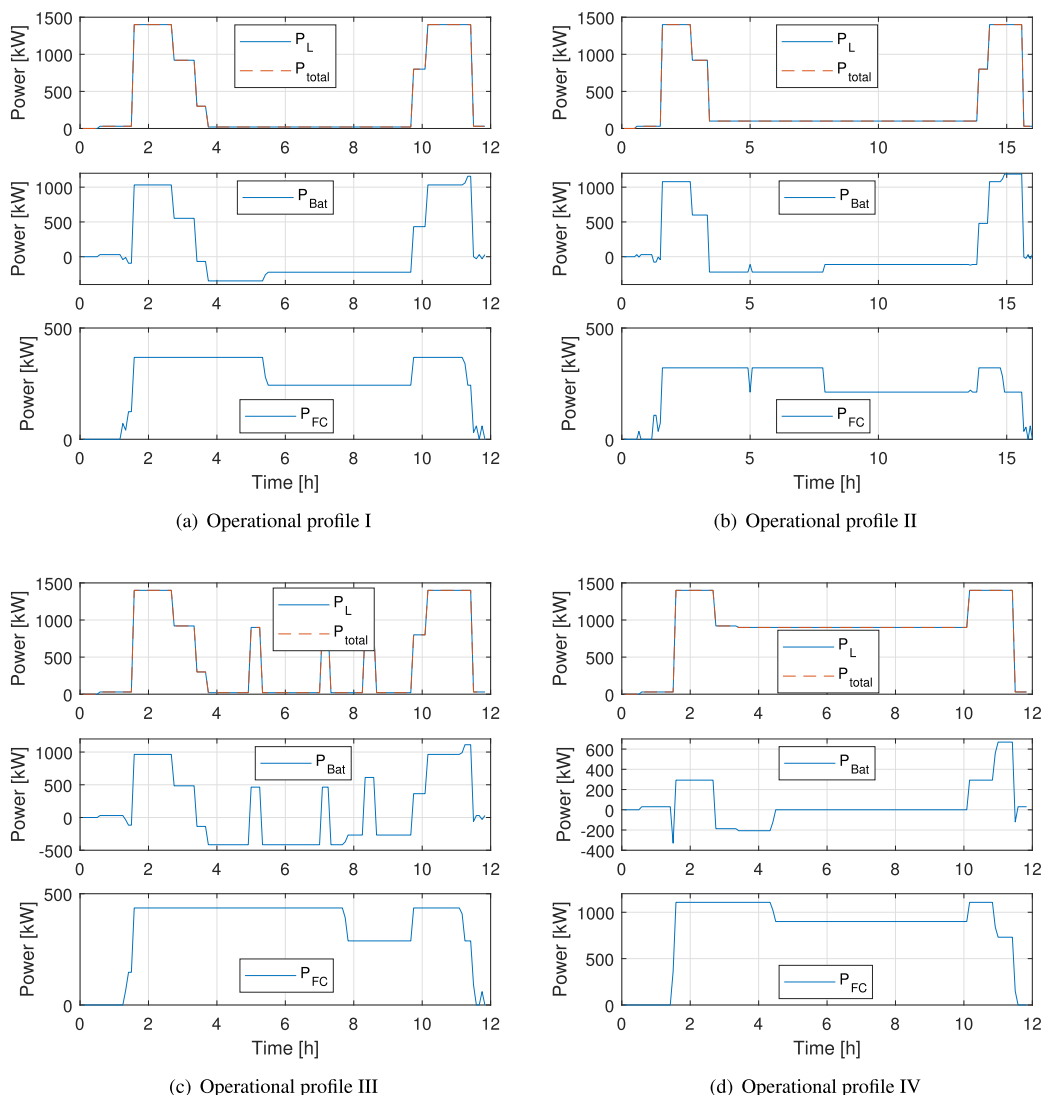
FIGURE 22. Power schedule of the selected designs for emission-free.

V. CONCLUSION

This paper applies a multi-objective double-layer optimization methodology to initially optimize the sizing and energy management of a hybrid ship propulsion system. Regarding the effects of the hybridization on the emission reduction, two main ranges are observed from the results of the studied offshore support vessel. In the low range of the emission reduction, the main reason is due to the efficiency improvement of the diesel engines. Only using the batteries to assist the engines is more cost-effective and practical to achieve a small emission reduction target (e.g. around 10% in this case study). In the high range, the emission reduction mainly depends on the amount of the hydrogen and the on-shore electricity consumed for the propulsion. This agrees with our expectations, but be proved by the optimized results presented in this paper.

Regarding the design guidelines for roughly sizing the power sources, for the small emission reduction target as mentioned above, the diesel engines provide most of the maximal power for the going and returning voyages. The batteries

either provide the whole power making the engines shut down in the low energy demand case (e.g. the operational profiles I and III) or operate alternatively with the engines making them run at higher power in the large energy demand case (e.g. the operational profiles II and IV). For the medium emission reduction target (e.g. ~50%), the diesel engines and the batteries each provide approximately half of the maximal power for the going and returning trips while the fuel cells provide a relatively low and roughly constant power during the whole voyage. One exception is the operation profile IV of high power and energy demand. In that case, the diesel engines and the fuel cells each provide approximately half of the maximal power and the batteries are sized accordingly. For the emission-free target, the power rating of the fuel cells could be roughly determined by the average power. The batteries could then be sized according to the maximal power and the energy demand. It would be good to mention that the exact solutions with specific ratings in this paper might not be available in the market. However, those initial sizing solutions leads to the initial design guidelines at the early design stage.

APPENDIX
OPTIMIZATION CONSTRAINTS
A. DIESEL ENGINES

By using the piecewise linear approximation, the analytical representation of the fuel consumption rate can be formulated as:

$$f_{DF}^i \approx s_1 P_{DE_1}^i(t) + s_2 P_{DE_2}^i(t) + s_3 P_{DE_3}^i(t) + M_{DF_0}^i. \quad (17)$$

The original single variable $P_{DE}^i(t)$ is then replaced by three variables $P_{DE_1}^i(t)$, $P_{DE_2}^i(t)$ and $P_{DE_3}^i(t)$ given by:

$$P_{DE}^i(t) = P_{DE_1}^i(t) + P_{DE_2}^i(t) + P_{DE_3}^i(t). \quad (18)$$

Therefore, the constraint of the diesel engine (11) used in MILP is modified by the following three constraints.

$$0 \leq P_{DE_1}^i(t) \leq P_1^i, \quad (19)$$

$$0 \leq P_{DE_2}^i(t) \leq P_2^i - P_1^i, \quad (20)$$

$$0 \leq P_{DE_3}^i(t) \leq P_{DE}^r - P_2^i. \quad (21)$$

Due to the convexity of the approximated piecewise linear function, it is guaranteed that $P_{DE}^i(t)$ is scheduled in such a way that the low incremental slope segment will be scheduled first. In other words, this prevents the operation of $P_{DE_3}^i(t) \neq 0$ while $P_{DE_2}^i(t) = 0$, for instance.

B. FUEL CELLS

By using the piecewise linear approximation, the analytical representation of (10) can be formulated as:

$$f_{FC}^k \approx s_1 P_{FC_1}^k(t) + s_2 P_{FC_2}^k(t) + s_3 P_{FC_3}^k(t) + P_{FC_0}^k. \quad (22)$$

The single variable $P_{FC}^k(t)$ can be replaced by three variables given by:

$$P_{FC}^k(t) = P_{FC_1}^k(t) + P_{FC_2}^k(t) + P_{FC_3}^k(t). \quad (23)$$

Then, the constraint of the fuel cells (15) used in MILP is modified by the following three constraints.

$$0.1 \cdot P_{FC}^r \leq P_{FC_1}^k(t) \leq P_1^k, \quad (24)$$

$$0 \leq P_{FC_2}^k(t) \leq P_2^i - P_1^k, \quad (25)$$

$$0 \leq P_{FC_3}^k(t) \leq 0.9 \cdot P_{FC}^r - P_2^k. \quad (26)$$

C. DEMAND SUPPLY

The constraint of the demand supply given by (16) is updated as:

$$P_L(t) = \sum_{i=1}^{N_{DE}} \sum_{m=1}^{3} P_{DE_m}^i(t) \cdot X_{DE_m}^i(t)$$
$$+ \sum_{j=1}^{N_{Bat}} P_{Bat}^j(t) \cdot X_{Bat}^j(t) + \sum_{k=1}^{N_{FC}} \sum_{n=1}^{3} P_{FC_n}^k(t) \cdot X_{FC_n}^k(t). \quad (27)$$

REFERENCES

[1] D. Kumar and F. Zare, "A comprehensive review of maritime microgrids: System architectures, energy efficiency, power quality, and regulations," *IEEE Access*, vol. 7, pp. 67249–67277, 2019.

[2] S. Faber, S. Hanayama, and S. Zhang, "Fourth IMO GHG study 2020—Final report," Int. Maritime Organisation (IMO), London, U.K., Tech. Rep., Jul. 2020. [Online]. Available: https://wwwcdn.imo.org/localresources/en/OurWork/Environment/Documents/Fourth%20IMO%20GHG%20Study%202020%20-%20Full%20report%20and%20annexes.pdf

[3] E. Skjong, R. Volden, E. Rødskar, M. Molinas, T. A. Johansen, and J. Cunningham, "Past, present, and future challenges of the marine vessel's electrical power system," *IEEE Trans. Transport. Electrific.*, vol. 2, no. 4, pp. 522–537, Dec. 2016.

[4] B. Zahedi, L. E. Norum, and K. B. Ludvigsen, "Optimized efficiency of all-electric ships by DC hybrid power systems," *J. Power Sources*, vol. 255, pp. 341–354, Jun. 2014.

[5] J. J. Valera-García and I. Atutxa-Lekue, "On the optimal design of hybrid-electric power systems for offshore vessels," *IEEE Trans. Transport. Electrific.*, vol. 5, no. 1, pp. 324–334, Mar. 2019.

[6] O. Alnes, S. Eriksen, and B.-J. Vartdal, "Battery-powered ships: A class society perspective," *IEEE Electrific. Mag.*, vol. 5, no. 3, pp. 10–21, Sep. 2017.

[7] J. Hou, J. Sun, and H. F. Hofmann, "Mitigating power fluctuations in electric ship propulsion with hybrid energy storage system: Design and analysis," *IEEE J. Ocean. Eng.*, vol. 43, no. 1, pp. 93–107, Jan. 2018.

[8] C. E. Thomas, "Fuel cell and battery electric vehicles compared," *Int. J. Hydrogen Energy*, vol. 34, no. 15, pp. 6005–6020, Aug. 2009.

[9] K. Ogawa, T. Yamamoto, H. Hasegawa, and T. Furuya, "Development of the fuel-cell/battery hybrid railway vehicle," in *Proc. IEEE Vehicle Power Propuls. Conf.*, Dearborn, MI, USA, Sep. 2009, pp. 1730–1735.

[10] M. Banaei, M. Rafiei, J. Boudjadar, and M.-H. Khooban, "A comparative analysis of optimal operation scenarios in hybrid emission-free ferry ships," *IEEE Trans. Transport. Electrific.*, vol. 6, no. 1, pp. 318–333, Mar. 2020.

[11] B. Bendjedia, N. Rizoug, M. Boukhnifer, and F. Bouchafaa, "Hybrid fuel cell/battery source sizing and energy management for automotive applications," *IFAC-PapersOnLine*, vol. 50, no. 1, pp. 4745–4750, Jul. 2017.

[12] M. Carignano, V. Roda, R. Costa-Castelló, L. Valino, A. Lozano, and F. Barreras, "Assessment of energy management in a fuel cell/battery hybrid vehicle," *IEEE Access*, vol. 7, pp. 16110–16122, 2019.

[13] J. Han, J.-F. Charpentier, and T. Tang, "An energy management system of a fuel cell/battery hybrid boat," *Energies*, vol. 7, no. 5, pp. 2799–2820, Apr. 2014.

[14] L. van Biert, M. Godjevac, K. Visser, and P. V. Aravind, "A review of fuel cell systems for maritime applications," *J. Power Sources*, vol. 327, pp. 345–364, Sep. 2016.

[15] J. Han, J. F. Charpentier, and T. Tang, "State of the art of fuel cells for ship applications," in *Proc. IEEE Int. Symp. Ind. Electron.*, May 2012, pp. 1456–1461.

[16] R. D. Geertsma, R. R. Negenborn, K. Visser, and J. J. Hopman, "Design and control of hybrid power and propulsion systems for smart ships: A review of developments," *Appl. Energy*, vol. 194, pp. 30–54, May 2017.

[17] B. Kawasieckyi, "Efficiency analysis and design methodology of hybrid propulsion systems," M.S. thesis, Dept. Maritime Transp. Technol., TU Delft, Delft, The Netherlands, 2013.

[18] S. Jafarzadeh and I. Schjølberg, "Operational profiles of ships in norwegian waters: An activity-based approach to assess the benefits of hybrid and electric propulsion," *Transp. Res. D, Transp. Environ.*, vol. 65, pp. 500–523, Dec. 2018.

[19] E. Silvas, T. Hofman, A. Serebrenik, and M. Steinbuch, "Functional and cost-based automatic generator for hybrid vehicles topologies," *IEEE/ASME Trans. Mechatronics*, vol. 20, no. 4, pp. 1561–1572, Aug. 2015.

[20] E. Silvas, T. Hofman, N. Murgovski, L. F. P. Etman, and M. Steinbuch, "Review of optimization strategies for system-level design in hybrid electric vehicles," *IEEE Trans. Veh. Technol.*, vol. 66, no. 1, pp. 57–70, Jan. 2017.

[21] T. Hofman, M. Steinbuch, R. van Druten, and A. Serrarens, "Design of CTV-based hybrid passenger cars," *IEEE Trans. Veh. Technol.*, vol. 58, no. 2, pp. 572–578, Feb. 2009.

[22] W. Gao and C. Mi, "Hybrid vehicle design using global optimization algorithms," *Int. J. Elect. Hybrid Veh.*, vol. 1, no. 1, pp. 57–70, 2007.

[23] T. Donateo, L. Serrao, and G. Rizzoni, "A two-step optimization method for the preliminary design of a hybrid electric vehicle," *Int. J. Elect. Hybrid Veh.*, vol. 1, no. 2, pp. 142–165, Apr. 2008.

[24] E. Silvas, E. Bergshoeff, T. Hofman, and M. Steinbuch, "Comparison of bi-level optimization frameworks for sizing and control of a hybrid electric vehicle," in *Proc. IEEE Vehicle Power Propuls. Conf. (VPPC)*, Oct. 2014, pp. 1–6.

[25] E. Skjong, T. A. Johansen, M. Molinas, and A. J. Sørensen, "Approaches to economic energy management in diesel–electric marine vessels," *IEEE Trans. Transport. Electrific.*, vol. 3, no. 1, pp. 22–35, Mar. 2017.

[26] C. Shang, D. Srinivasan, and T. Reindl, "Economic and environmental generation and voyage scheduling of all-electric ships," *IEEE Trans. Power Syst.*, vol. 31, no. 5, pp. 4087–4096, Sep. 2016.

[27] F. D. Kanellos, G. J. Tsekouras, and N. D. Hatziargyriou, "Optimal power management with GHG emissions limitation in all-electric ship power systems comprising energy storage systems," *IEEE Trans. Power Syst.*, vol. 5, no. 4, pp. 1166–1175, Oct. 2014.

[28] A. Boveri, P. Gualeni, D. Neroni, and F. Silvestro, "Stochastic approach for power generation optimal design and scheduling on ships," in *Proc. IEEE PES Innov. Smart Grid Technol. Conf. Eur. (ISGT-Eur.)*, Torin, Italy, Sep. 2017, pp. 1–6.

[29] S. Mashayekh, Z. Wang, L. Qi, J. Lindtjorn, and T.-A. Myklebust, "Optimum sizing of energy storage for an electric ferry ship," in *Proc. IEEE Power Energy Soc. General Meeting*, Torin, Italy, Jul. 2012, pp. 1–8.

[30] B. A. Skinner, P. R. Palmer, and G. T. Parks, "Multi-objective design optimisation of submarine electric drive systems," in in *Proc. IEEE Elect. Ship Technol. Symp*, May 2007, pp. 65–71.

[31] B. A. Skinner, G. T. Parks, and P. R. Palmer, "Comparison of submarine drive topologies using multiobjective genetic algorithms," *IEEE Trans. Veh. Technol.*, vol. 58, no. 1, pp. 57–68, Jan. 2009.

[32] W. Zhang, A. Maleki, A. K. Birjandi, M. Alhuyi Nazari, and O. Mohammadi, "Discrete optimization algorithm for optimal design of a solar/wind/battery hybrid energy conversion scheme," *Int. J. Low-Carbon Technol.*, pp. 1–15, Sep. 2020.

[33] D. Lloyd, "Handbook for maritime and offshore battery systems," DNV GL, Bærum, Norway, Tech. Rep. 2016-1056, 2016.

[34] E. Catillo, A. J. Gonejo, P. Pedregal, R. Garciá, and N. Alguacil, *Building and Solving Mathematical Programming Models in Engineering and Science*. Hoboken, NJ, USA: Wiley, 2001.

[35] J. Nocedal and S. Wright, *Numerical Optimization*. New York, NY, USA: Springer, 2006.

[36] X. Wang, T. D. Strous, D. Lahaye, H. Polinder, and J. A. Ferreira, "Modeling and optimization of brushless doubly-fed induction machines using computationally efficient finite-element analysis," *IEEE Trans. Ind. Appl.*, vol. 52, no. 6, pp. 4525–4534, Nov. 2016.

[37] K. Deb, A. Pratap, S. Agarwal, and T. Meyarivan, "A fast and elitist multi objective genetic algorithm: NSGA-II," *IEEE Trans. Evol. Comput.*, vol. 6, no. 2, pp. 182–197, Apr. 2002.

[38] W. Shi, H. T. Grimmelius, and D. Stapersma, "Analysis of ship propulsion system behaviour and the impact on fuel consumption," *Int. Shipbuild. Prog.*, vol. 57, nos. 1–2, pp. 35–64, 2010.

[39] G. Liu, "Generation scheduling for power systems with demand response and a high penetration of wind energy," Ph.D. dissertation, Dept. Elect. Eng. Comput. Sci., Univ. Tennessee, Knoxville, TN, USA, 2014.

XUEZHOU WANG (Member, IEEE) received the B.Sc. and M.Sc. degrees in electrical engineering from Northwestern Polytechnical University, Xi'an, China, in 2010 and 2013, respectively, and the Ph.D. degree in electrical engineering from the Delft University of Technology, Delft, The Netherlands, in 2017. From 2017 to 2020, he worked as a Senior Electromagnetic Design Engineer with Envision Energy, Shanghai, China. He is currently working as a Postdoctoral Researcher in hybrid drivetrain systems for ship applications with the Delft University of Technology. His current research interests include modeling and design of electrical machines, novel generators for wind turbines, and transportation electrification.

UDAI SHIPURKAR received the Ph.D. degree from the Delft University of Technology, The Netherlands, in 2019. He was a Postdoctoral Researcher with the Maritime and Transport Technology Department, TU Delft, where he worked on hybrid power and propulsion systems for ships. Since 2020, he has been with MARIN, where he is involved in modeling engine rooms of the future and applying model based system engineering to the conceptual design of power, propulsion, and energy systems. His research interest includes modeling and control of marine systems.

ALI HASELTALAB is currently a Postdoctoral Researcher with the Delft University of Technology, where he working towards enabling fuel-efficient and emission free autonomous shipping. As a Researcher with the Department of Maritime and Transport Technology and the Researchlab Autonomous Shipping (RAS), he is involved in several projects related to Minimized Emissions Autonomous Shipping. His current research interests include control of marine systems, power and propulsion systems analysis and control, and multi-agent control of transport systems.

HENK POLINDER (Senior Member, IEEE) received the Ph.D. degree in electrical engineering from the Delft University of Technology, Delft, The Netherlands, in 1998. Since 1996, he has been an Assistant/Associate Professor with the Delft University of Technology, working in the field of electrical machines and drives. He worked part-time in industries, at wind turbine manufacturer Lagerwey, from 1998 to 1999; Philips CFT, in 2001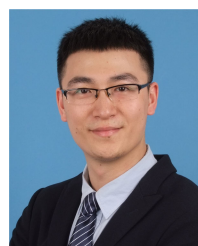; and ABB Corporate Research, Västerås, in 2008. He was a Visiting Scholar with Newcastle University, Newcastle upon Tyne, in 2002; Laval University, Quebec, in 2004; The University of Edinburgh, in 2006; and the University of Itajubá, in 2014. He has authored or coauthored of over 250 publications. His main research interests include electric drive and energy systems for maritime applications and offshore renewables.

FRANS CLAEYS received the master's degree in electrotechnical engineering from KU Leuven, in 1982. His main expertise is in the design and implementation of algorithms for hydrographic survey data acquisition and processing, the positioning and attitude sensors, such as GNSS and FOGs, seaborne or airborne sensors, such as lidar, multispectral, thermal sensors, and digital cameras on movable platforms, and the execution of hydrographic surveys using a wide range of survey aperture. As a Research and Development Manager of GEO Group of Companies, he supports projects related to greenhouse gas emissions reduction and hybrid propulsion powertrains.

RUDY R. NEGENBORN is currently a Full Professor in multi-machine operations and logistics. He is also the Head of the Department Maritime and Transport Technology, Section of Transport Engineering and Logistics, and the Researchlab Autonomous Shipping. His work has been published in over 200 peer reviewed academic publications. His research interests include multi-agent systems, distributed control, model predictive control, simulation of large-scale transport systems, and applications in networked transport systems. He is also an Editor of the books, such as *Intelligent Infrastructures*, *Distributed Model Predictive Control Made Easy*, and *Transport of Water Versus Transport Over Water: Exploring the Dynamic Interplay of Transport and Water*.

• • •